

Bis-imidazole ring-containing bipolar organic small molecule cathodes for high-voltage and ultrastable lithium-ion batteries

Liping Zheng^{a,b}, Jiayi Ren^d, Huige Ma^{b,c}, Mingsheng Yang^d, Xiaorong Yan^d, Rui Li^{b,c}, Qian Zhao^d, Jianze Zhang^{a,b}, Haifeng Fu^f, Xiong Pu^{a,b,c}, Mingjun Hu^{*,d}, Jun Yang^{**},
b,c,e

^aSchool of Chemistry and Chemical Engineering, Center on Nanoenergy Research, Guangxi University, Nanning 530004, China.

^bBeijing Institute of Nanoenergy and Nanosystems, Chinese Academy of Sciences, Beijing 101400, China. E-mail: yangjun@binn.cas.cn

^cSchool of Nanoscience and Technology, University of Chinese Academy of Sciences, Beijing, 100049, China.

^dSchool of Materials Science and Engineering, Beihang University, Beijing 100191, China. E-mail: mingjunhu@buaa.edu.cn

^eShenzhen Institute for Advanced Study, University of Electronic Science and Technology of China, Shenzhen 518000, China.

^fBeijing Electromechanical Research Institute Co. Ltd., Beijing 100083, China.

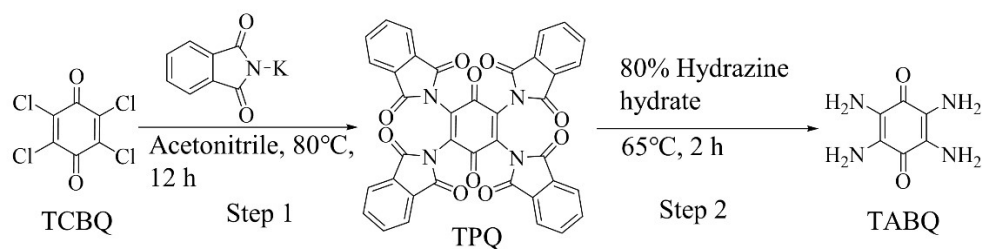
S1 Experimental section

S1.1 Materials

All the reagents (Chloranil (98%, Macklin), potassium phthalimide (99%, Boer), acetonitrile (99.8%, Boer), N,N-Dimethylformamide 99%, Macklin), hydrazine hydrate (98%, Aladdin), ethanol (99.8%, Macklin), 4-(N,N-Diphenylamino) benzaldehyde (99.38%, Bidepharm), acetic acid (99.5%, Macklin)) were used directly without any processing.

S1.2 The synthesis of TABQ

The TABQ was obtained according to a previously reported method as described in Scheme S1¹.



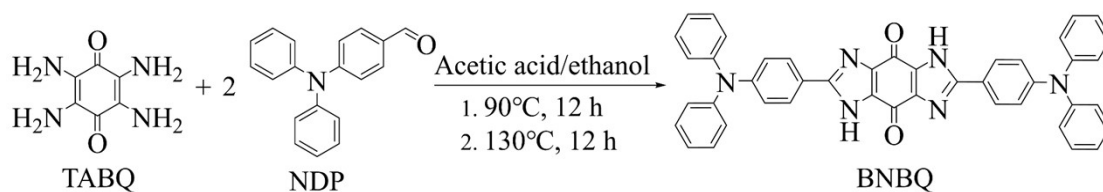
Scheme S1. Synthetic routes for TABQ

Step 1: 5.0 g (0.02 mol) of Chloranil (TCBQ), 15.0 g (0.80 mol) of potassium phthalimide, and 50.0 mL of acetonitrile were added into a 100 mL two-necked flask. The mixture was kept at 80 °C for 12 h under stirring. After cooling to room temperature, the solid was separated by vacuum filtration and rinsed several times with N,N-Dimethylformamide and boiling water. The product was dried at 80 °C overnight, and brown-yellow powder of tetra(phthalimido)-benzoquinone (TPQ) was obtained (11.4 g, yield = 80.7%).

Step 2: 9.41 g (0.014 mol) of TPQ was added to 200 mL of 80% hydrazine hydrate in a 500 mL three-neck round bottom flask. The mixture was stirred at room temperature for 2 h, followed by heating at 65 °C for 2 h. The mixture was cooled to room temperature, filtered under vacuum, washed several times with water and ethanol, and the dark purple product of TABQ was obtained (1.2 g, yield = 56.5%). ¹H NMR, (500 MHz, [D₆] DMSO): δ 4.55 (s, 8H) (Figure S1a).

S1.3 The synthesis of BNBQ

The synthesis of BNBQ involving a Schiff-based solvothermal condensation reaction was summarized in Scheme S2².



Scheme S2. Synthetic routes for BNBQ.

Typically, 0.81 g of 4-(N,N-Diphenylamino) benzaldehyde (NDP) was added in acetic acid/ethanol (25 mL, 1:1 /vol.). 0.25 g of TABQ was added to the above solution. After stirring for 60 minutes under nitrogen, the reaction mixture slowly heated up to 90 °C for 12 h, and then react at 130 °C for 12 h. The reaction was quenched by adding 20 ml of water to the flask. The maroon suspension was collected and thoroughly washed several times with ethanol and deionized water, then recrystallized in the ethanol. Finally, the products were obtained by vacuum drying at 65 °C overnight (yield = 62%). HRMS (APCI)⁺ m/z calculated for C₄₄H₃₀N₆O₂ [M+H]⁺: 675; found: 675.2495 (Figure S2a), Elemental Analysis calculated for C₄₄H₃₀N₆O₂: C 78.32%, H 4.48%, N

12.46%, O 4.83%; found: C 73.66%, H 4.67%, N 12.53%, O 9.42% (Table S1).

S2 Characterization

The crystal structures of BNBQ was attained by powder X-ray diffraction (PXRD, Thermo Scientific Escalab 250Xi) with a 2θ range from 5° to 80° . Fourier-transform infrared (FT-IR) spectroscopy was recorded on a Thermo Scientific Nicolet iS50 spectrometer with a single reflection ATR accessory (ZnS crystal) from $400\text{-}4000\text{ cm}^{-1}$, and liquid $^1\text{H-NMR}$ spectrum (Bruker AVANCE III HD 500 MHz, solvent: dimethyl sulfoxide- d_6 , chloroform- d_6) were used to confirm the structure of TABQ and BNBQ, respectively. Elemental content was explored through elemental analysis (EA) using a Elementar Unicube organic element analyzer. Material morphology was characterized by scanning electron microscopy (FEI Nova Nano SEM, American). X-ray photoelectron spectroscopy (XPS) was attained using Thermo Scientific Escalab 250Xi. Thermogravimetric analysis (TGA) was performed using a Rigaku TG/DTA8122 thermogravimetric analyzer at a ramping rate of $10^\circ\text{C min}^{-1}$ to 900°C at the atmosphere of N_2 . High-resolution mass spectrometry (HRMS) was performed with a QExactive Focus mass spectrometer (Thermo Scientific, USA, solvent: dichloromethane) to verify the molecular weight.

S3 Electrochemical measurements

All organic cathodes were manufactured by mixing the active materials (BNBQ), Ketjen black (KB, ECP-600JD), and binder (polyvinylidene fluoride, PVDF) in N-methylpyrrolidone (NMP) to form a well-dispersed slurry at a thickness of $34 \pm 2\ \mu\text{m}$ by using doctor blade technique, which was subsequently coated on aluminum foil and dried in a vacuum oven at 60°C overnight. The weight ratio of active materials, KB, and PVDF in the cathode pellets were 6:3:1 (for the cycle performance test at 1000 mA g^{-1} , the mass ratio was 5:4:1, and 6:3:1 (Figure S10a), respectively). The mass of the active material loading of all electrodes was $0.75 \pm 0.15\text{ mg cm}^{-2}$ (for sodium-ion half-cells, the mass loading was $0.75\text{-}0.90\text{ mg cm}^{-2}$). After weighing the electrode sheets, the electrodes were made into a half-cell lithium battery using a CR2032 type coin cell assembly, and pure lithium foil was used as the counter electrode (sodium-ion half-cells, pure sodium foil was used as the counter electrode). 1.0 M LiPF_6 in a mixture of ethylene carbonate (EC) and dimethyl carbonate (DEC) (1:1 v/v) was used as the electrolyte in an argon-filled glove box (concentrations of O_2 and $\text{H}_2\text{O} < 1\text{ ppm}$), and 1.0 M LiTFSI in 1,2-dimethoxyethane (DME) and 1,3-dioxolane (DOL) (1:1 v/v) was applied as the electrolyte for TABQ electrode (1.0 M NaClO_4 in EC and DEC (1:1

vol%) with 5.0% 4-Fluoro-1,3-dioxolan-2-one as the electrolyte for sodium-ion half-cells). Meanwhile, polypropylene membrane (Celgard 2400) was used as a separator. The assembled battery sat at room temperature for about 10 hours. Then the galvanostatic charge and discharge measurements of the assembled cells were performed on a LANHE battery testing system (CT3001A) in the voltage range of 2.0-4.2 V at different current densities. The cyclic voltammetry (CV) measurements were performed on CHI 660E electrochemical workstation (Chen Hua, Shanghai). EIS was also conducted via CHI 660E with the frequency ranging from 10 mHz to 100 kHz at room temperature.

S4 The calculation of theoretical capacity and energy density

Theoretical capacity C_t (mAh g⁻¹) was calculated based on the equation³:

$$C_t = \frac{nF}{3600(Mw/1000)} = \frac{26801n}{Mw}$$

where n and Mw were the transfer number of charge carriers and the molecular weight of the active material, respectively. And the molecular weight of BNBQ (C₄₄H₃₀N₆O₂) was calculated to be = 675 g mol⁻¹. The transfer number of electrons (n) involved in the unit was 6. Therefore, the theoretical capacity C_t was 238 mAh g⁻¹ for BNBQ (N-type capacity contribution: 79 mAh g⁻¹, P-type capacity contribution: 159 mAh g⁻¹). Similarly, the theoretical capacity of NDP was 98 mAh g⁻¹, and 318 mAh g⁻¹ for TABQ.

The energy density (E) could be calculated using the following equation:

$E = C_{\text{capacity}} \times V_{\text{average}}$, where C_{capacity} was the discharge specific capacity and V_{average} was the average discharge potential (vs. Li/Li⁺).

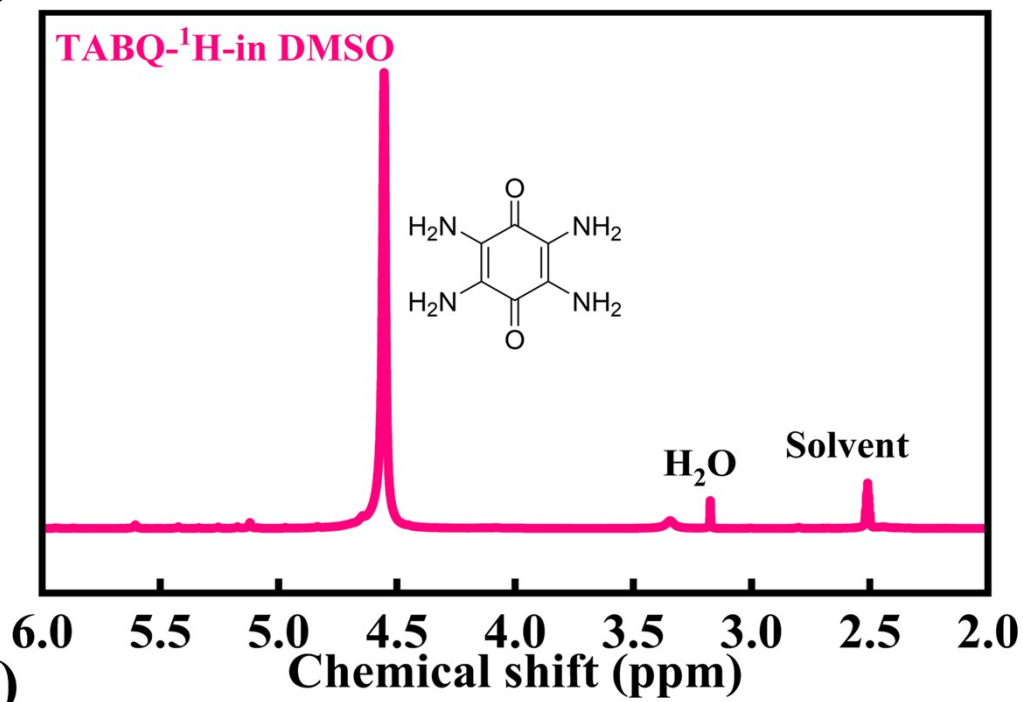
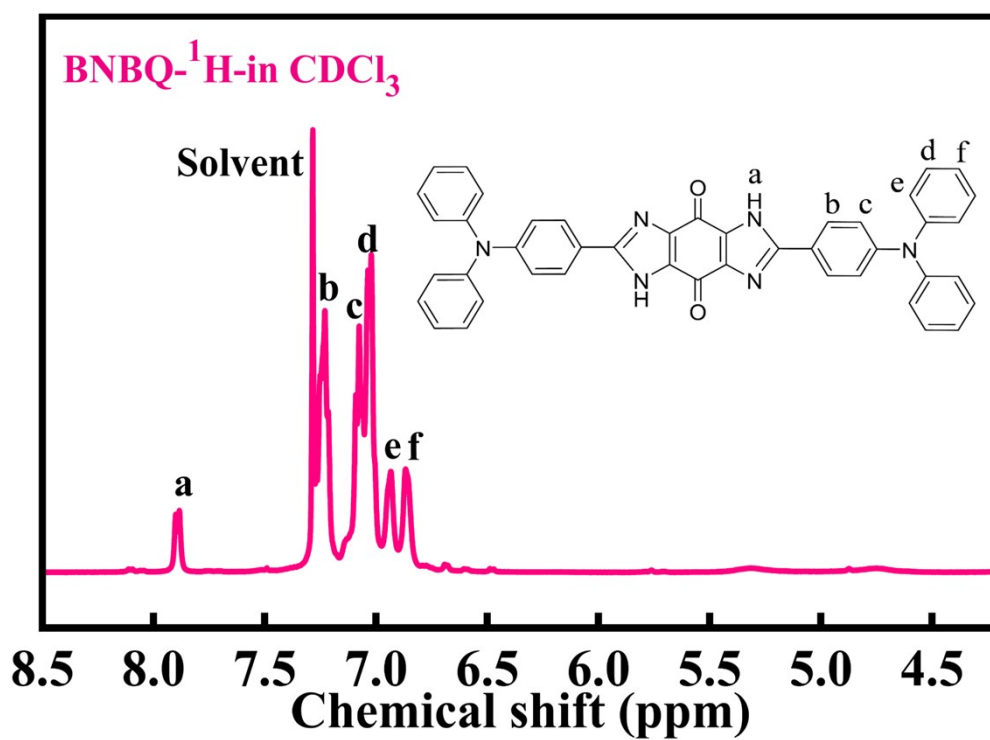
(a)**(b)**

Figure S1. (a) ¹H NMR spectra (DMSO, 500 MHz) of TABQ, (b) ¹H NMR spectra (CDCl₃, 500 MHz) of BNBQ.

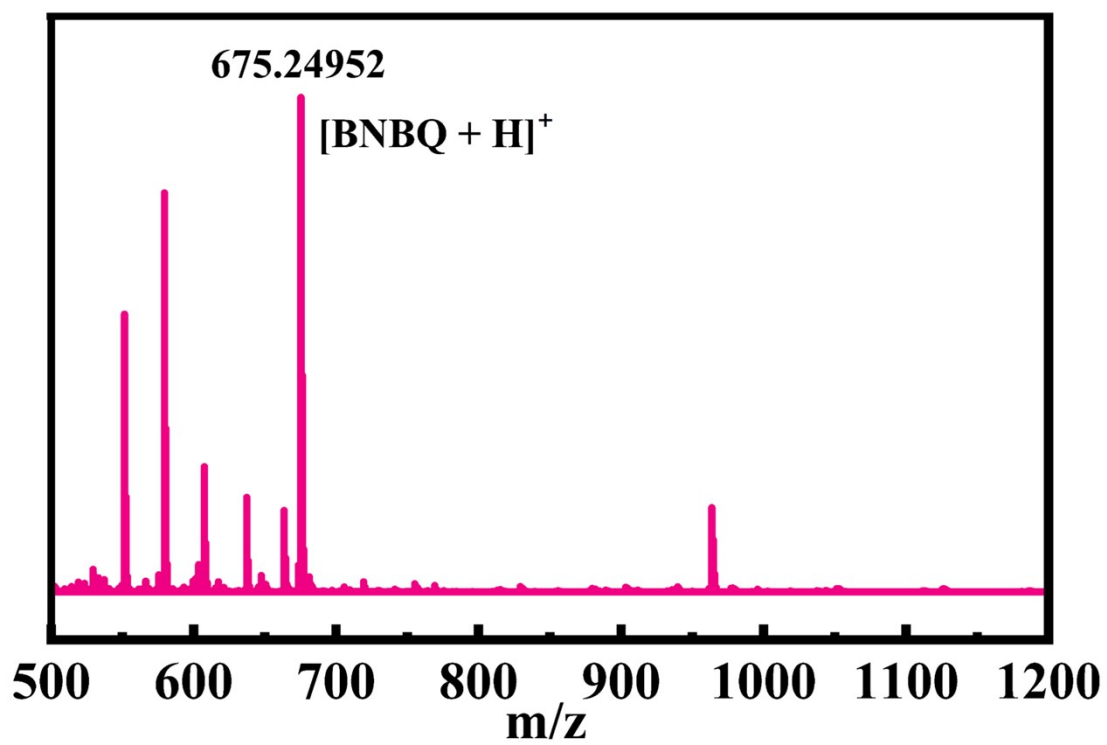


Figure S2. HRMS spectra (CH₂Cl₂) of BNBQ.

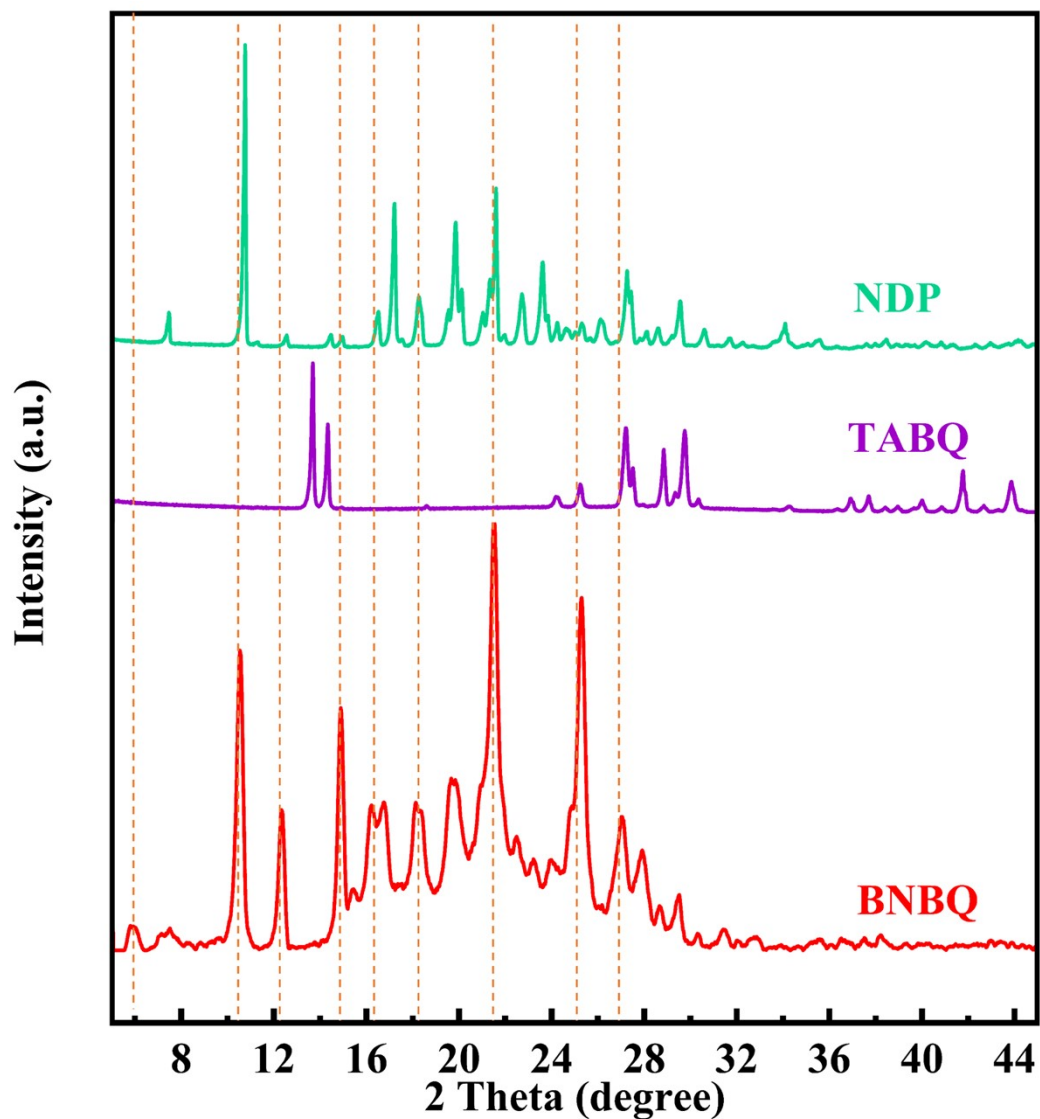


Figure S3. XRD patterns of BNBQ, TABQ and NDP, respectively.

Table S1. Elemental analysis of BNBQ.

	C	H	N	O
Estimated (wt %)	73.66	4.67	12.53	9.42
Theoretical (wt %)	78.32	4.48	12.46	4.83

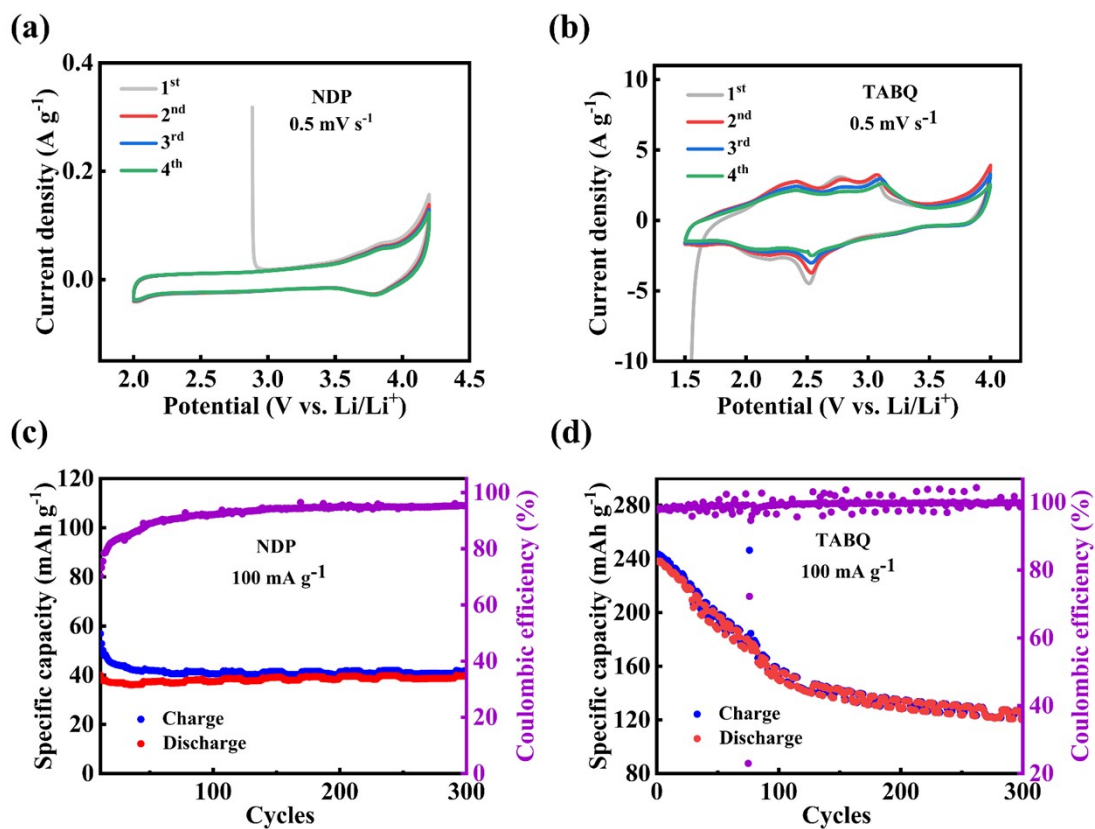


Figure S4. CV of (a) NDP and (b) TABQ, respectively; Cycling stability of (c) NDP and (d) TABQ electrodes at the current density of 100 mA g⁻¹. The utilization rate of active functional groups of NDP was only 40%, and 80% for TABQ.

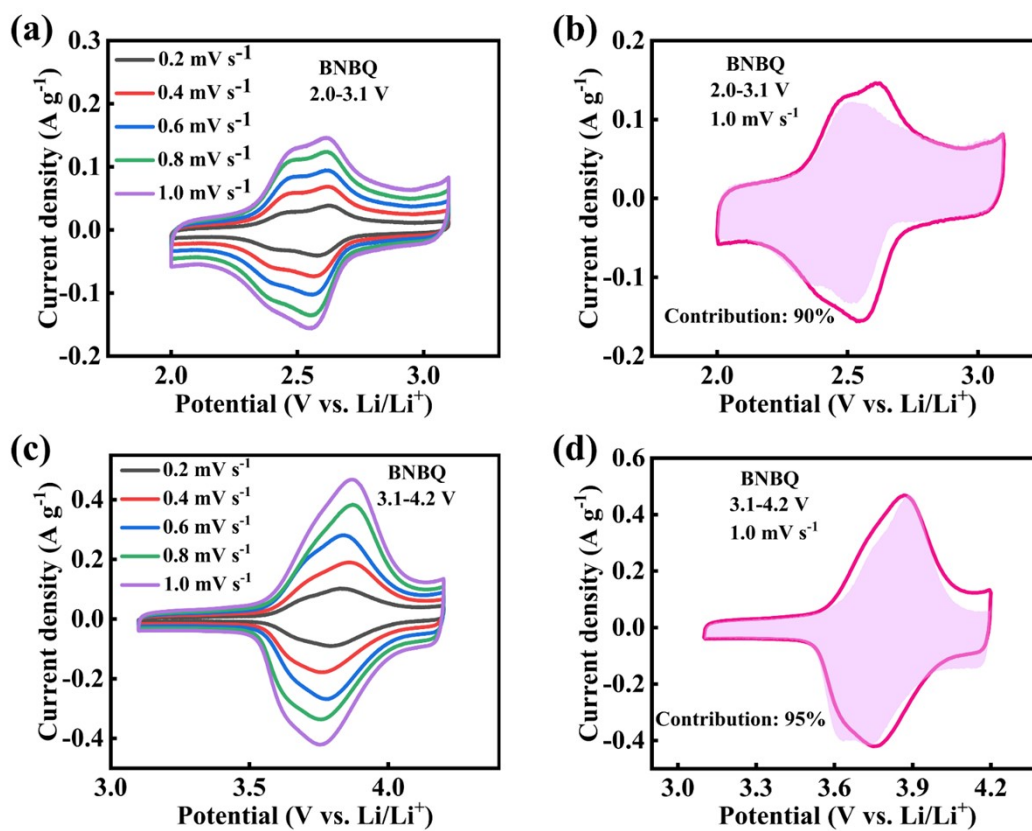


Figure S5. CV curves of BNBQ cathodes in different voltage ranges of (a) 2.0-3.1 V, and (b) 3.1-4.2 V at different scan rates.

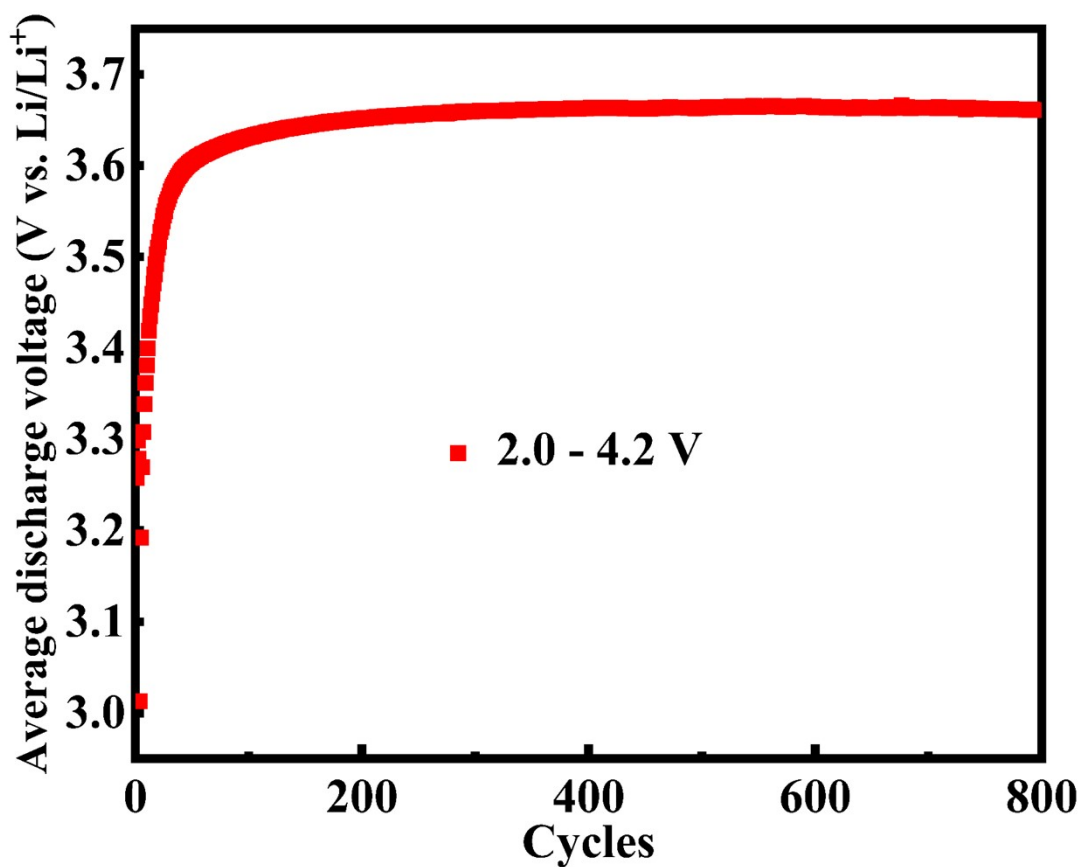


Figure S6. The average discharge voltages of BNBQ over 2.0-4.2 V (vs. Li/Li⁺).

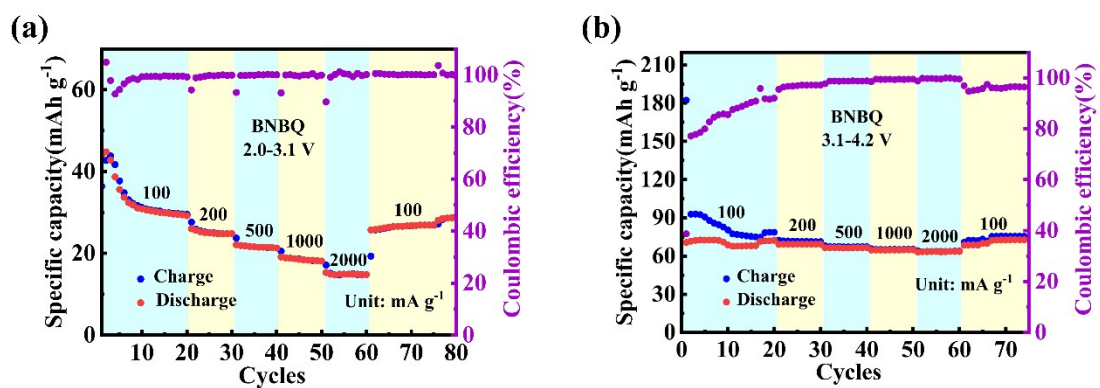


Figure S7. Rate performance of BNBQ cathodes in different voltage ranges of (a) 2.0-3.1 V, and (b) 3.1-4.2 V.

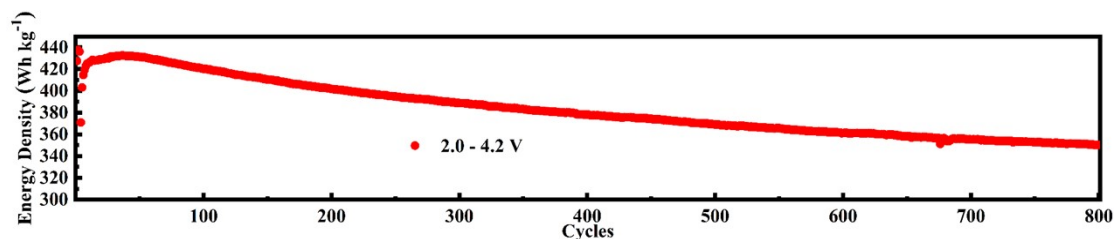


Figure S8. Energy densities of BNBQ over 2.0-4.2 V.

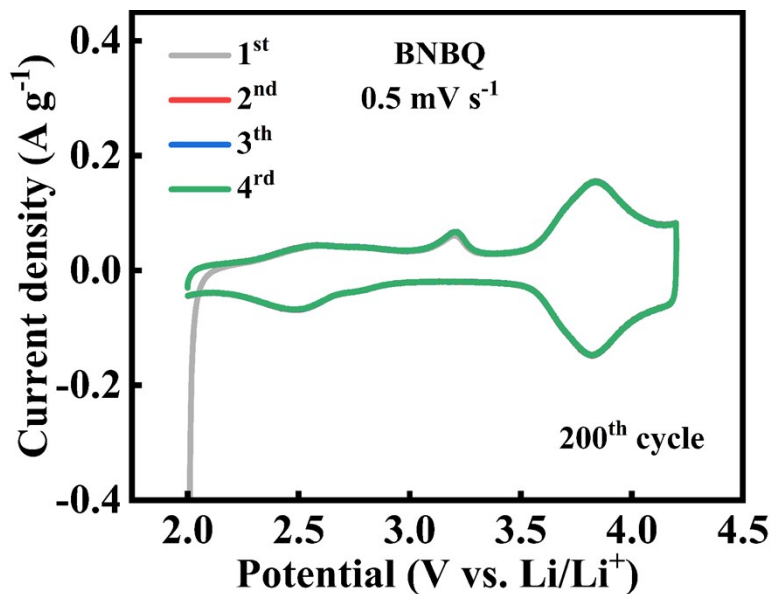


Figure S9. CV curves of BNBQ cathodes in the 200th cycle at 100 mA g⁻¹.

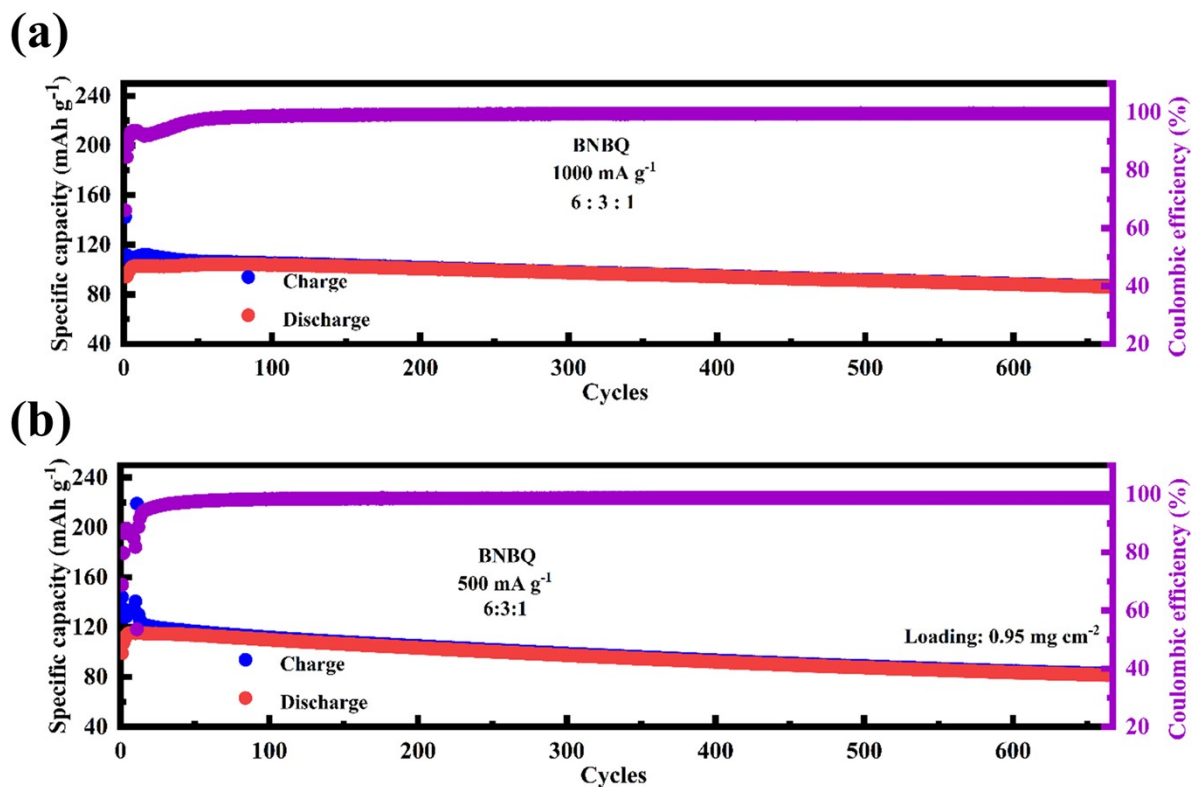


Figure S10. Cycling stability of BNBQ electrodes at the current density of (a) 1000 mA g⁻¹, and (b)

500 mA g⁻¹.

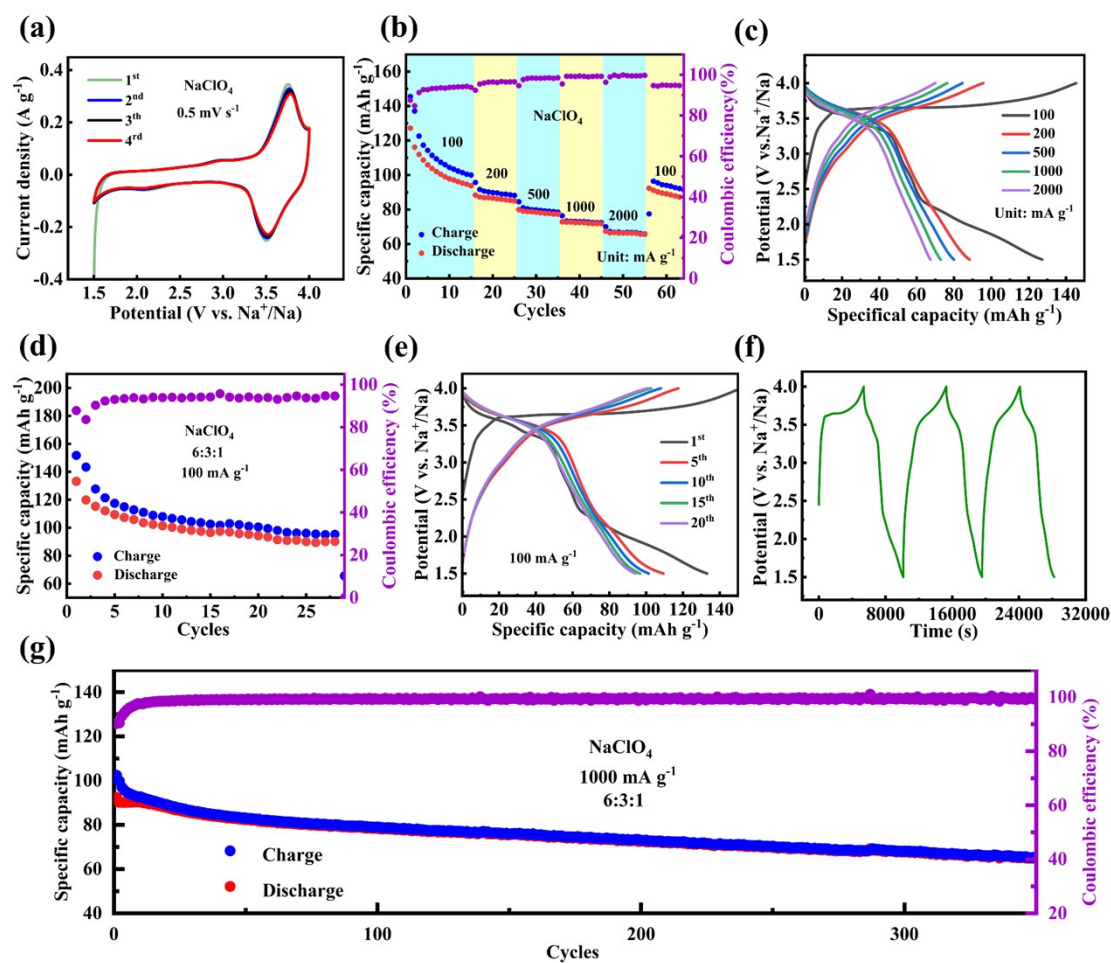


Figure S11. Electrochemical performance of BNBQ in sodium-ion batteries. (a) CV curves of BNBQ at 0.5 mV s⁻¹; (b) Rate performance of BNBQ in the 1.5-4.0 V voltage range at various current densities; (c) Charge/discharge profiles at varied current densities; (d) Long-term cycling stability of BNBQ at 100 mA g⁻¹; (e) Charge-discharge voltage profiles for BNBQ at 100 mA g⁻¹; (f) Charge-discharge profiles of BNBQ; (g) Cycling performance of BNBQ at 1000 mA g⁻¹.

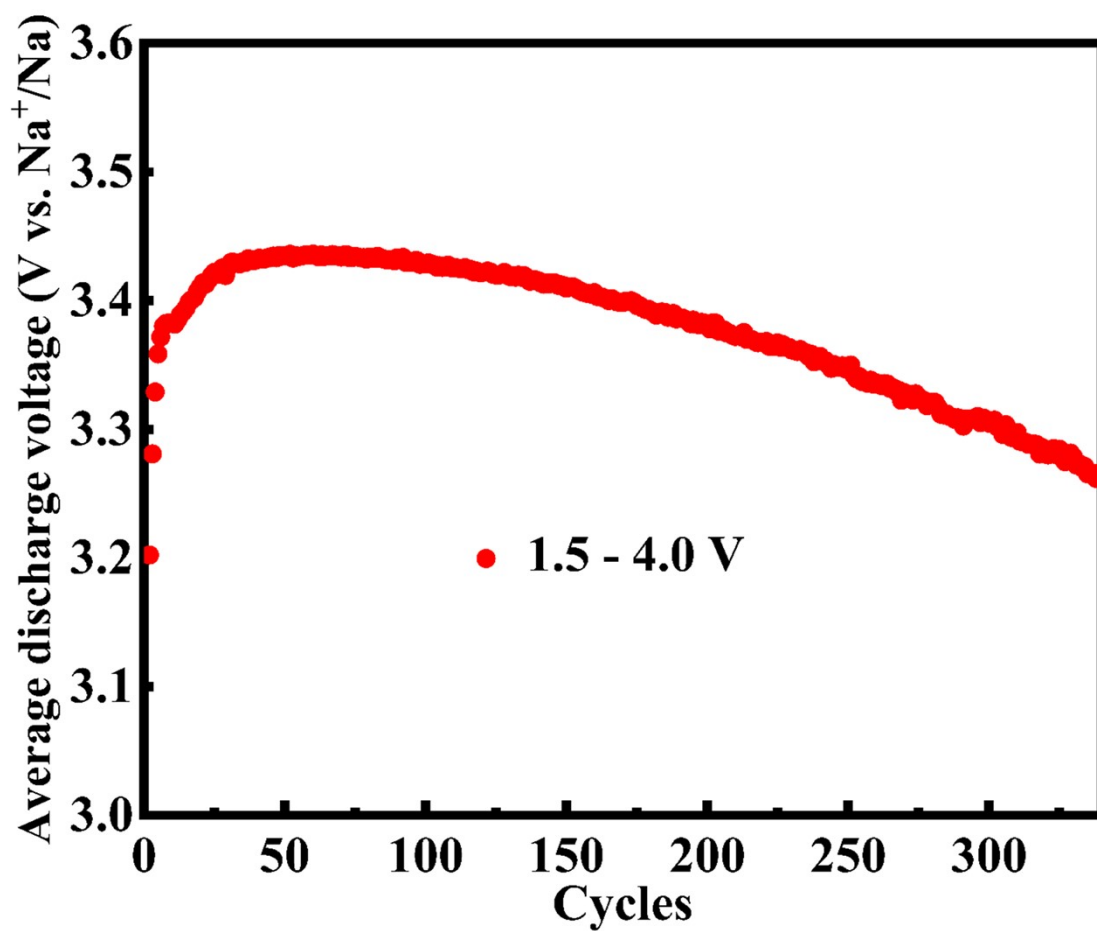


Figure S12. The change of the average discharge voltages of BNBQ (V vs. Na⁺/Na) with cycles in the range of 1.5-4.0 V.

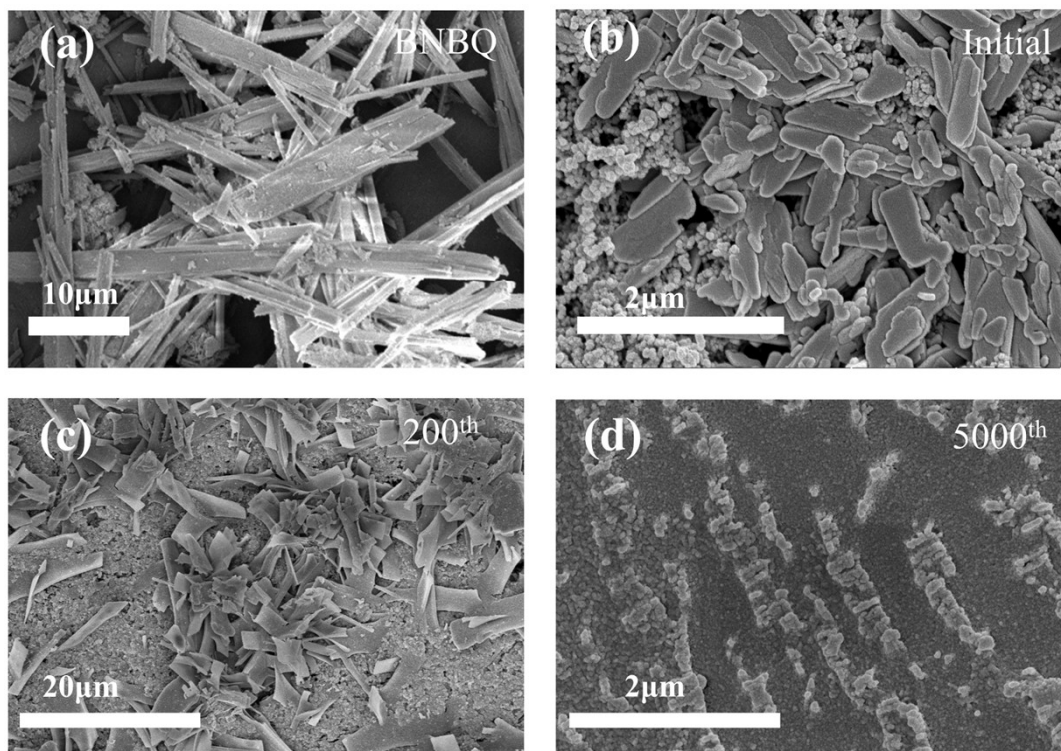


Figure S13. (a) SEM images of BNBQ; SEM images of BNBQ electrode at different electrochemical stages: (b) initial, (c) after 200 cycles at 100 mA g⁻¹, and (d) after 5000 cycles at 1000 mA g⁻¹.

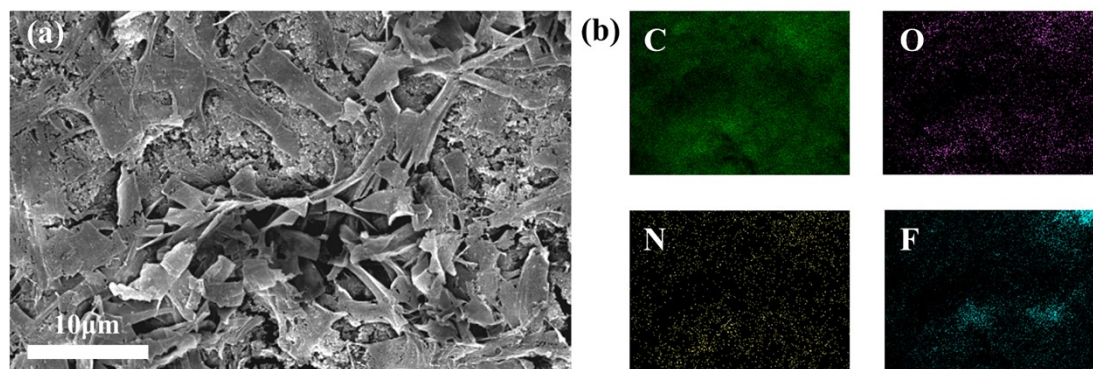


Figure S14. (a) SEM images of BNBQ electrode after 200 cycles at 100 mA g⁻¹ and (b) distribution diagram of elements.

Table S2. Electrochemical performance comparison of organic cathode materials in lithium batteries with high discharge voltage (>3.6 V) reported in the literature.

Compounds	Reversible capacity (mAh g ⁻¹)	Capacity retention (mAh g ⁻¹) @cycles@current density(A g ⁻¹)	The mass ratio of active agent, and binder	Discharge Voltage	Ref
PTEO	80	64@1000@1.47	1 8 1	3.7	4
PVK	99.4	--@100@1.2	5 4 1	3.9	5
P1	66	21@100@--	50 47 3	4.1	6
p-DPPZ	170	125@500@0.2	75 15 10	4.1/3.3	7
Coronene	40	40@4400@--	7 2 1	4.0	8
Perylene	90	50@1800@--	7 2 1	3.8/3.3	8
PPP	80	70@100@0.04	7 2 1	4.3/4.0	9
p-DPPZS	133	114@1000@0.83	75 15 10	3.8/3.1	10
TCTA	92	48@5000@1	63 27 10	3.95	11
pDPICZO	90	78@800@1.25	68 25 7	3.5–3.8 /4–4.4	12
3PXZ	112	73@100@0.129	40 40 20	3.7	13
DBTOP	108	--@100@0.6	5 4 1	3.87/4.3	14
BNBQ	133	70.1@5000@1	5 4 1	3.64	This work

References

1. Z. Lin, H. Y. Shi, L. Lin, X. Yang, W. Wu and X. Sun, *Nat Commun*, 2021, **12**, 4424.
2. P. R. Lakshmi, P. Jayasudha and K. P. Elango, *Spectrochim Acta A Mol Biomol Spectrosc*, 2019, **213**, 318-323.
3. M. Wu, Y. Zhao, B. Sun, Z. Sun, C. Li, Y. Han, L. Xu, Z. Ge, Y. Ren, M. Zhang, Q. Zhang, Y. Lu, W. Wang, Y. Ma and Y. Chen, *Nano Energy*, 2020, **70**, 104498.
4. K. Oyaizu, T. Kawamoto, T. Suga and H. Nishide, *Macromolecules*, 2010, **43**, 10382-10389.
5. J. Kim, H. S. Park, T. H. Kim, S. Y. Kim and H. K. Song, *Phys Chem Chem Phys*, 2014, **16**, 5295-5300.
6. M. E. Speer, M. Kolek, J. J. Jassoy, J. Heine, M. Winter, P. M. Bieker and B. Esser, *Chem Commun (Camb)*, 2015, **51**, 15261-15264.
7. G. Dai, X. Wang, Y. Qian, Z. Niu, X. Zhu, J. Ye, Y. Zhao and X. Zhang, *Energy Storage Materials*, 2019, **16**, 236-242.
8. I. A. Rodriguez-Perez, C. Bommier, D. D. Fuller, D. P. Leonard, A. G. Williams and X. Ji, *ACS Appl Mater Interfaces*, 2018, **10**, 43311-43315.
9. L. M. Zhu, A. W. Lei, Y. L. Cao, X. P. Ai and H. X. Yang, *Chem Commun (Camb)*, 2013, **49**, 567-569.
10. G. Dai, Y. Liu, Z. Niu, P. He, Y. Zhao, X. Zhang and H. Zhou, *Matter*, 2019, **1**, 945-958.
11. C. Zhao, Z. Chen, W. Wang, P. Xiong, B. Li, M. Li, J. Yang and Y. Xu, *Angew Chem Int Ed Engl*, 2020, **59**, 11992-11998.
12. G. Dai, Y. Gao, Z. Niu, P. He, X. Zhang, Y. Zhao and H. Zhou, *ChemSusChem*, 2020, **13**, 2264-2270.
13. K. Lee, I. E. Serdiuk, G. Kwon, D. J. Min, K. Kang, S. Y. Park and J. E. Kwon, *Energy & Environmental Science*, 2020, **13**, 4142-4156.
14. Y. Zheng, H. Ji, J. Liu, Z. Wang, J. Zhou, T. Qian and C. Yan, *Nano Lett*, 2022, **22**, 3473-3479.